ResearchGate

See discussions, stats, and author profiles for this publication at: https://www.researchgate.net/publication/273533970

Experimental evidence for competitive NO and OC bond homolysis in gas-phase alkoxyamines

ARTICLE *in* INTERNATIONAL JOURNAL OF MASS SPECTROMETRY · JULY 2014

Impact Factor: 1.97 · DOI: 10.1016/j.ijms.2014.06.030

READS

21

5 AUTHORS, INCLUDING:

Ganna Gryn'ova

École Polytechnique Fédérale de Lausanne

22 PUBLICATIONS **191** CITATIONS

SEE PROFILE

Michelle L Coote

Australian National University

214 PUBLICATIONS **5,679** CITATIONS

SEE PROFILE

Philip J Barker

University of Wollongong

32 PUBLICATIONS **393** CITATIONS

SEE PROFILE

All in-text references underlined in blue are linked to publications on ResearchGate, letting you access and read them immediately.

Available from: Ganna Gryn'ova
Retrieved on: 24 January 2016

International Journal of Mass Spectrometry 378 (2015) 38–47

Contents lists available at ScienceDirect

International Journal of Mass Spectrometry

journal homepage: www.elsevier.com/locate/ijms

Experimental evidence for competitive N—O and O—C bond homolysis in gas-phase alkoxyamines

David L. Marshall [a,b], Ganna Gryn'ova [b,c], Michelle L. Coote [b,c], Philip J. Barker [b,d], Stephen J. Blanksby [a,b,e,*]

[a] School of Chemistry, University of Wollongong, NSW 2522, Australia
[b] ARC Centre of Excellence for Free Radical Chemistry and Biotechnology, Australia
[c] Research School of Chemistry, Australian National University, Canberra, ACT 0200, Australia
[d] Bluescope Steel Research, PO Box 202 Port Kembla, NSW 2505, Australia
[e] Central Analytical Research Facility, Queensland University of Technology, QLD 4000, Australia

ARTICLE INFO

Article history:
Received 24 March 2014
Received in revised form 26 June 2014
Accepted 30 June 2014
Available online 2 July 2014

In honor of Prof. Veronica M. Bierbaum, friend and colleague, on the occasion of her 65th birthday.

Keywords:
Tandem mass spectrometry
Nitroxyl radical
Alkoxyamine
Bond homolysis

ABSTRACT

The extensive use of alkoxyamines in controlled radical polymerisation and polymer stabilisation is based on rapid cycling between the alkoxyamine ($R^1R^2NO—R^3$) and a stable nitroxyl radical ($R^1R^2NO^\bullet$) *via* homolysis of the labile O—C bond. Competing homolysis of the alkoxyamine N—O bond has been predicted to occur for some substituents leading to production of aminyl and alkoxyl radicals. This intrinsic competition between the O—C and N—O bond homolysis processes has to this point been difficult to probe experimentally. Herein we examine the effect of local molecular structure on the competition between N—O and O—C bond cleavage in the gas phase by variable energy tandem mass spectrometry in a triple quadrupole mass spectrometer. A suite of cyclic alkoxyamines with remote carboxylic acid moieties ($HOOC—R^1R^2NO—R^3$) were synthesised and subjected to negative ion electrospray ionisation to yield $[M-H]^-$ anions where the charge is remote from the alkoxyamine moiety. Collision-induced dissociation of these anions yield product ions resulting, almost exclusively, from homolysis of O—C and/or N—O bonds. The relative efficacy of N—O and O—C bond homolysis was examined for alkoxyamines incorporating different R^3 substituents by varying the potential difference applied to the collision cell, and comparing dissociation thresholds of each product ion channel. For most R^3 substituents, product ions from homolysis of the O—C bond are observed and product ions resulting from cleavage of the N—O bond are minor or absent. A limited number of examples were encountered however, where N—O homolysis is a competitive dissociation pathway because the O—C bond is stabilised by adjacent heteroatom(s) (*e.g.* $R^3 = CH_2F$). The dissociation threshold energies were compared for different alkoxyamine substituents (R^3) and the relative ordering of these experimentally determined energies is shown to correlate with the bond dissociation free energies, calculated by *ab initio* methods. Understanding the structure-dependent relationship between these rival processes will assist in the design and selection of alkoxyamine motifs that selectively promote the desirable O—C homolysis pathway.

© 2014 Elsevier B.V. All rights reserved.

1. Introduction

Hindered amine light stabilisers (HALS) are anti-oxidant additives employed to improve the durability and lifetime of polymer surface coatings in outdoor applications [1,2]. Even at low concentrations, inclusion of HALS improves gloss and colour retention in pigmented coatings and provides a superior aesthetic for the lifetime of the product. Despite the clear advantages offered by their usage, the exact role of HALS in stabilising polymer coatings remains an active topic of discussion [3–11]. Contemporary mechanisms for this anti-oxidant action invoke cycling of the amine functional group of the HALS between the alkoxyamine ($R^1R^2NO—R^3$), nitroxyl radical ($R^1R^2NO^\bullet$, variously referred to as 'nitroxide' or 'aminoxyl'), and aminyl radical ($R^1R^2N^\bullet$) forms (Scheme 1a) [12]. The stable nitroxyl radical scavenges deleterious polymer chain-based macroradicals ($R^{3\bullet}$), which otherwise accelerate polymer degradation through chain scission. The combination product is an alkoxyamine containing the polymer fragment bonded directly to the nitroxide. Advantageously, nitroxyl radicals are subsequently regenerated from these alkoxyamines, and

* Corresponding author. Present address: Central Analytical Research Facility, Institute for Future Environments, Queensland University of Technology, Brisbane, QLD 4000, Australia. Tel.: +61 73138 3343.
E-mail address: stephen.blanksby@qut.edu.au (S.J. Blanksby).

http://dx.doi.org/10.1016/j.ijms.2014.06.030
1387-3806/© 2014 Elsevier B.V. All rights reserved.

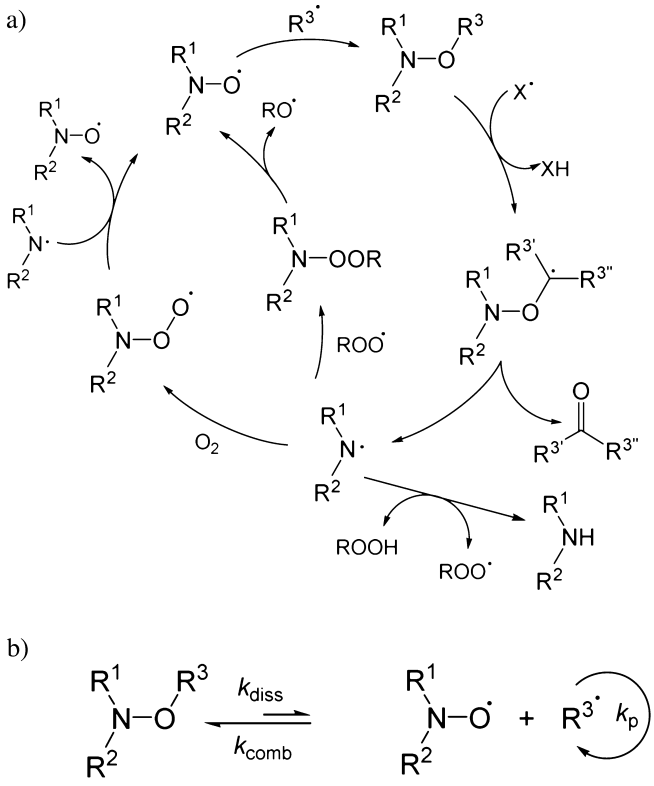

Scheme 1. (a) Polymer stabilisation activity of HALS by regenerative cycling of nitroxyl radicals, as described by contemporary computational cycle involving β-hydrogen abstraction from an alkoxyamine and an aminyl radical intermediate [12]; (b) simplified mechanism of nitroxide mediated polymerisation, highlighting reversible O—C bond formation and homolysis (k_{comb}, k_{diss}, and k_p represent the rates of combination, dissociation, and propagation, respectively).

by-products of the reformation step are relatively inert. While direct cleavage of the O—C and N—O bonds directly connects the alkoxyamine with both the nitroxyl and aminyl radicals, under typical service conditions homolysis pathways are not energetically competitive with an alternative mechanism that involves a β-hydrogen elimination step and connects these intermediates within the catalytic cycle [12–14]. Nevertheless, the impact of the R^3-substituent, which varies widely depending on the polymer substrate and breakdown mechanism, on the relative energetics of the O—C and N—O bonds remains of considerable interest [15].

Alkoxyamines are similarly central to the mechanism of nitroxide-mediated polymerisation (Scheme 1b), a technique that produces materials with low polydispersity and controlled molecular weight [16,17]. However, the success of nitroxide-mediated polymerisation depends on control over the reversibility and rates of alkoxyamine formation and dissociation, as well as suppressing the significance of side-reactions, such as disproportionation. These factors in turn are dependent on the structure of both the nitroxide and the monomer [18,19]. Driven by the importance of reversible O—C bond homolysis to both polymer synthesis and stabilisation, the molecular structural factors governing such a step in alkoxyamines are well characterised [20–28]. Conversely, less attention has been paid to the unwanted corresponding N—O cleavage, which would result in the formation of highly reactive aminyl and alkoxyl radicals. Homolysis of the N—O bond in alkoxyamines is promoted when either or both of the resulting radicals are stabilised. For example, N—O bond homolysis is observed during degradation of indoline-based nitroxides, whereby the homolysis product is an aryl aminyl radical [29–31], and in thermolysis of alkoxyamines with aryl or acyl *O*-ether substituents [32–35]. In a theoretical study of the competitive bond cleavage processes [36], Tordo and co-workers demonstrated that, whilst semi-empirical computational methods reliably predict relative trends in the O—C bond dissociation energies (BDEs) of a series of alkoxyamines [14], higher level density functional methods are required to adequately describe the competition between the O—C and N—O cleavage processes. A more recent comprehensive theoretical study [15], using benchmarked high-level *ab initio* methods, established that certain alkoxyamine functionalities (*i.e.* R^3 in Scheme 1) promote N—O homolysis over O—C homolysis due to anomeric stabilisation of the O—C bond [37]. Gigmes and co-workers have suggested that "there may be a competition between (N)O—C and N—O(C) bond cleavage. The possibility and the extent of bond cleavage depend on the nature of the R^3 alkyl moiety bound to the *O*-atom of the nitroxide function" [29]. Testing this hypothesis experimentally for the intrinsic dissociation of alkoxyamines in the gas phase is the central aim of this work.

Tandem mass spectrometry is a well-established approach to investigate competing mechanisms of dissociation in gas-phase ions. If the charged moiety is largely fixed within the molecular scaffold and is isolated from the labile functional groups, then it is possible to observe charge-remote dissociation, which may be closely related to thermolysis of analogous neutral species [38–40]. It has previously been demonstrated that alkoxyamines undergo charge-remote homolysis of the O—C bond [41–43]. For example, Oh and co-workers derivatised small peptides with alkoxyamines [44–46] and subjected these to electrospray ionisation (ESI) to form ions with the charge sites localised to amino acid residues and thus remote from the alkoxyamine. Subsequent collision-induced dissociation (CID) of these ions resulted in almost exclusive O—C bond homolysis, generating an alkyl radical which initiated further fragmentation of the peptide ion. However, depending on the nature and proximity of the charge to the alkoxyamine moiety, bond homolysis is not always selectively observed, and ions resulting from charge-directed fragmentation may also be present [47,48]. Building on this understanding we have developed a molecular scaffold incorporating an alkoxyamine functional group carrying a wide range of R^3-subsituents and a remote negative charge to experimentally investigate competition between charge-remote O—C and N—O homolysis during low-energy CID. Further experimental and computational approaches verify the structure-dependent energetics of the competing N—O and O—C homolysis processes, and highlight the local structural requirements for N—O homolysis in alkoxyamines.

2. Material and methods

2.1. Materials

Nitroxyl radicals 4-carboxy-2,2,6,6-tetramethylpiperidine-1-oxyl (4-carboxy-TEMPO, **1**) and 3-carboxy-2,2,5,5-tetramethylpyrrolidine-1-oxyl (3-carboxy-PROXYL, **2**) were purchased from Sigma–Aldrich (Sydney, Australia), and used without further purification. Hydrogen peroxide (Australian Chemical Reagents, Queensland, Australia) was used as a 40% (w/w) aqueous solution. Perdeuterated (D_6)-acetone was purchased from Cambridge Isotope Laboratories (Andover, MA, USA). Methanol employed for mass spectrometry was HPLC grade (Thermo Fisher Scientific, Melbourne, Australia) and used as received. All other materials for synthesis were purchased from Sigma–Aldrich, and used as received.

2.2. Synthesis

Synthesis of alkoxyamines from nitroxide precursors and various alkyl radical sources has been widely documented [49–54]. Alkoxyamines (with the exception of **1c** and **1e**) were

prepared according to the method of Schoening et al. [55,56], whereby alkyl radicals are generated *in situ* from a ketone or aldehyde, copper (I) chloride, and hydrogen peroxide. In the presence of the nitroxide, nascent radicals are readily trapped, forming the desired alkoxyamines, listed in Scheme 2. This method was chosen for its simplicity, ready availability of reagents, and wide array of possible functionalities, with the exception of benzaldehydes, which do not generate phenyl radicals under these conditions. **1c** was prepared by substituting TEMPO for 4-carboxy-TEMPO (**1**) in a literature method, refluxing overnight in cyclohexene [57,58]. Preparation of **1e** was also based on adaptation of an existing method, refluxing 4-carboxy-TEMPO (**1**) and the radical initiator 1,1′-azobis(cyclohexanecarbonitrile) for 30 h in methanol [59]. 4-*N*,*N*,*N*,-Trimethylamino-TEMPO was prepared as the iodide salt according to the method of Strehmel et al. [60]. Characterisation of all products by high-resolution mass spectrometry is provided as Supporting Information (Table S1).

2.3. Mass spectrometry

Negative ion mass spectra were recorded with a QuattroMicro (Waters, Manchester, U.K.) triple quadrupole mass spectrometer equipped with an ESI source and controlled by Micromass MassLynx software (version 4.1). Alkoxyamines (Scheme 2) were diluted to *ca.* 5 μM in methanol, and infused directly into the ESI source at 5 μL min^{-1}. The capillary voltage was set to 3.0 kV, cone voltage 25 V, and source temperature 80 °C. Nitrogen was used as the drying gas, at a temperature of 110 °C, and flow rate of 320 L h^{-1}. In all collision induced dissociation (CID) scans, ions of interest were selected in Q1, subjected to collisions with argon gas in Q2 at a pressure of 3.0 ± 0.1 mTorr, and the collision energy in the laboratory frame (E_{lab}) was varied from 2 to 25 eV. For product ion structural validation, MS^n spectra were recorded on an LTQ 2-dimensional linear ion trap mass spectrometer (Thermo Fisher Scientific, San Jose, CA, USA), and high-resolution MS and MS/MS spectra were acquired on a Waters Xevo G1 Q-ToF mass spectrometer.

Breakdown curves are obtained by plotting the normalised intensity of the product ion(s) of interest against the collision energy in the centre-of-mass frame (E_{cm}), where E_{cm} is equal to E_{lab} multiplied by the reduced mass of the colliding ion and neutral argon gas. Empirically, threshold behaviour was analysed by using a least-squares fitting criterion to fit sigmoid functions to the data, of the type shown in Eq. (1) [61,62].

$$I_i(E_{cm}) = \frac{BR_i}{1 + e^{(E_{1/2,i} - E_{cm})b_i}} \quad (1)$$

In Eq. (1), BR_i is the branching ratio of the product ion of interest (i), $E_{1/2,i}$ is the energy at which the function has reached half of its maximum value, and the parameter b_i describes the steepness of the sigmoid curve. Furthermore, we define "dissociation threshold" as the energy at which the product ion abundance is equal to 5% of the total ion intensity (*i.e.* $I_i = 0.05$). As we are comparing fragmentation onsets and not quantitatively deriving energetic thresholds, we find that using the appearance energy definition of Schröder et al. [61,62] (*i.e.* using a linear extrapolation of the sigmoid curve at $E_{1/2}$ to the x-axis) does not significantly improve the quality of the data fit or the correlation with calculated thermodynamic quantities.

2.4. Computational procedures

Standard *ab initio* molecular orbital theory and density functional theory calculations were carried out using Gaussian 09 [63] and MOLPRO 2012.1 [64]. Calculations were performed at a high level of theory, recently demonstrated to predict gas- and solution-phase bond dissociation energies and associated equilibrium constants to within chemical accuracy [15,65]. Geometries of all species were fully optimised at the M06-2X/6-31 + G(d) level of theory. For all species, full systematic conformational searches (at a resolution of 60°) were carried out to ensure global, and not merely local, minima were located. Frequencies were calculated at this level and scaled by recommended scale factors [66]. Improved energies for all species were calculated using a double layer ONIOM-type method. The core layer (including both the nitroxyl and carboxylic acid moieties) was calculated using composite high-level G3(MP2,CC)(+) level of theory [67], where (+) denotes inclusion of diffuse functions in a standard 6-31G(d) basis set. The full system was calculated with the M06-2X/6-31 + G(d) method. This methodology has been shown to accurately predict the gas-phase energetics of nitroxyl and other free radical reactions [65,68]. Entropies and thermal corrections at 25, 80, and 110 °C were calculated using standard formulae for the statistical thermodynamics of an ideal gas under the harmonic oscillator approximation in conjunction with the optimised geometries and scaled frequencies [69].

3. Results and discussion

Alkoxyamines are readily detected as protonated or alkali metal adduct ions by electrospray ionisation (ESI) [48], matrix assisted laser desorption ionisation (MALDI) [70,71], liquid extraction surface analysis (LESA) [72], or desorption electrospray ionisation

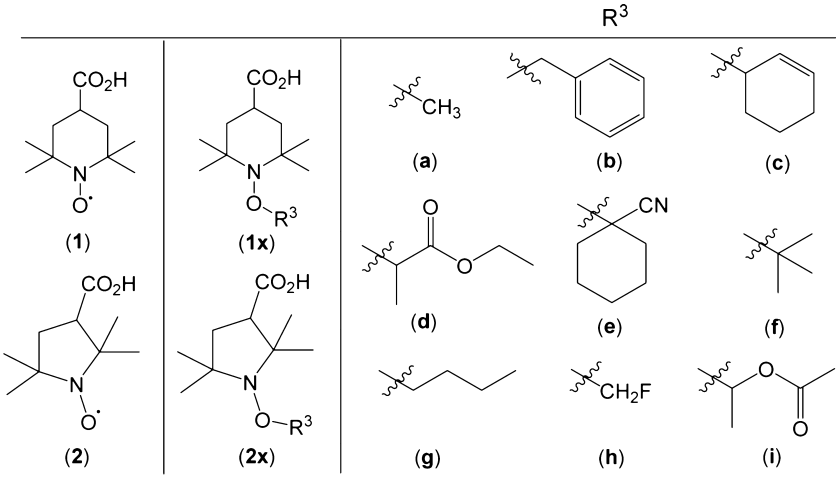

Scheme 2. Alkoxyamines (**1x**) and (**2x**) examined in this study, based on 4-carboxy-TEMPO (**1**) and 3-carboxy-PROXYL (**2**), where **x** is any R^3 group (**a–i**).

(DESI) [73]. However, in the absence of another basic moiety, protonation of an alkoxyamine nitrogen raises the O—C BDE by over 100 kJ mol^{-1} [74]. Charge-driven dissociation mechanisms dominate upon CID of $[M+H]^+$ or $[M+Na]^+$ alkoxyamine ions, leading to predictable and readily assignable products in the resulting spectra [41,48], but no information is ascertained concerning the relative energies of the N—O and O—C bonds. Our first attempts to produce charge-remote alkoxyamines were based on 4-*N,N,N*-trimethylamino-TEMPO, in order to sequester the charge on the piperidine fragment and promote homolysis. However, the CID spectra of such alkoxyamines (Supporting Information, Fig. S1) feature predominantly protonated *O*-alkyl acetone oxime fragment ions, and $[M-59]^+$ ions corresponding to loss of trimethylamine. The former dissociation is consistent with previous reports on the charge-directed dissociation of substituted piperidines [72]. In the absence of the desired charge-remote dissociation of the alkoxyamine moiety, an alternative strategy was sought. Only limited examples in the literature describe the tandem mass spectrometric analysis of alkoxyamines upon negative ion electrospray ionisation [46]. Commercially available nitroxides 4-carboxy-TEMPO (**1**) and 3-carboxy-PROXYL (**2**) were found to be suitable scaffolds for producing $[M-H]^-$ anions for the suite of TEMPO-based alkoxyamines designated **1a–i** and the PROXYL-series **2a, 2b** and **2h** (Scheme 2).

3.1. Dissociation of methoxyamines

Methanolic solutions of alkoxyamines displayed in Scheme 2 exhibit abundant $[M-H]^-$ ions upon negative ion ESI. These anions were isolated and subjected to CID in a triple quadrupole mass spectrometer using argon as the collision gas. Comparative CID spectra of methoxyamines **1a** and **2a** are displayed in Fig. 1(a) and (b), respectively. The most abundant product ion in each example represents a loss of 15 Da from the precursor ion and is assigned to the neutral loss of a methyl radical ($^{\bullet}CH_3$); a deviation from the 'even-electron rule' [75,76].

To demonstrate that the loss of 15 Da arises solely from O—C homolysis and not by ejection of a methyl radical from the piperidine ring, selective replacement of hydrogen with deuterium on the methoxyamine moiety was undertaken by using D_6-acetone in the synthesis of **2a** to form the isotopologue (D_3-methyl)-**2a**. Isolation and fragmentation of the $[M-H]^-$ ion at *m/z* 203, under the same experimental conditions, yields an abundant ion at *m/z* 185 representing a loss of 18 Da and ejection of D_3-methyl radical ($^{\bullet}CD_3$) (Fig. 1c). Importantly, no $[M-H-15]^-$ ions are observed at *m/z* 188 suggesting the methyl loss pathways occurs exclusively *via* O—C bond cleavage. For further confirmation, CID experiments were repeated on a linear ion-trap mass spectrometer with MS^n capabilities. Upon isolation and collisional activation of the *m/z* 185 product ions from both **2a** (Fig. 1b) and D_3-**2a** (Fig. 1c), the resulting spectra are identical, and moreover, identical to the MS^2 CID spectrum of the $[M-H]^-$ ion of a 3-carboxy-PROXYL (**2**) standard (Fig. 2b). Similarly, the MS^3 spectrum of the *m/z* 199 product ion from **1a** is identical to the MS^2 spectrum of 4-carboxy-TEMPO (**1**) (vide infra). The $[M-H-15]^-$ product ions at *m/z* 199 and *m/z* 185 for **1a** and **2a** respectively, correspond to loss of a methyl radical exclusively *via* homolysis of the O—C bond and are therefore assigned as the deprotonated nitroxyl radicals 4-carboxy-TEMPO (**1**) and 3-carboxy-PROXYL (**2**), respectively.

Closer examination of the CID spectra in Fig. 1 reveals further similarities in the precursor ion dissociation pattern. In Fig. 1(a) and (b), additional ions constituting neutral losses of 30, 31 and 46 Da in both spectra indicate that the predominant fragmentation pattern is common to both the 6- and 5-membered ring alkoxyamines. In Fig.1(c), the corresponding losses from the deuterium-labelled precursor ion are increased by 3 Da (*i.e.* 33, 34 and 49 Da). That is, the product ions at *m/z* 170, 169 and 154 are observed in both Fig. 1(b) and (c), indicating that none of these ions contain the methyl group from the methoxyamine.

The MS^2 spectrum of *m/z* 199 from authentic, deprotonated 4-carboxy-TEMPO (**1**) is identical to the MS^3 spectrum of *m/z* 199 from prior dissociation of **1a** (Fig. 2a). Collisional activation of *m/z* 199 ions (either from standard **1** or prior dissociation of **1a**) yields predominantly ions at *m/z* 184, indicating that methyl radical ejection also occurs from the nitroxide radical. These data suggest that the ions observed at *m/z* 184 in Fig. 1(a) are likely to come from

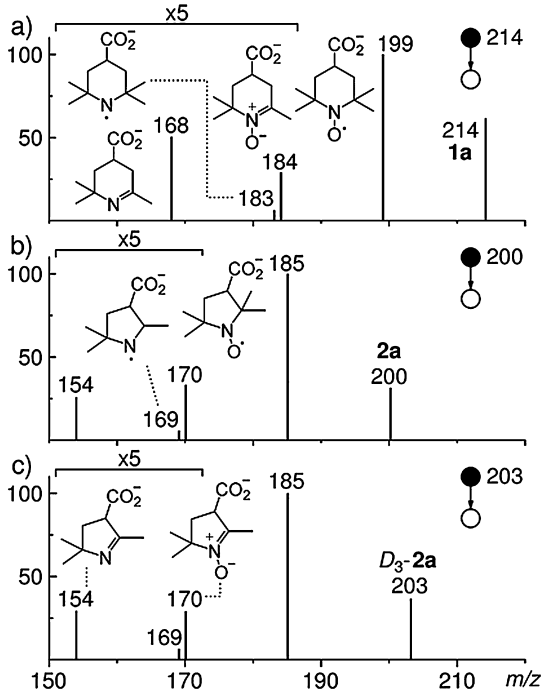

Fig. 1. Negative ion ESI-MS/MS spectra (at a laboratory frame collision energy of 15 eV) of the $[M-H]^-$ ions; (a) **1a** at *m/z* 214, (b) **2a** at *m/z* 200, (c) (D_3-methyl)-**2a** at *m/z* 203. Peaks between *m/z* 150 and 190 (a), and between *m/z* 150 and 175 (b and c) have been magnified by a factor of 5.

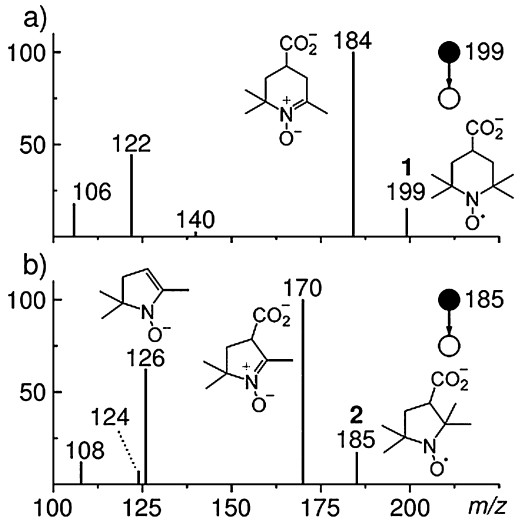

Fig. 2. CID spectra of $[M-H]^-$ ions of authentic: (a) 4-carboxy-TEMPO (**1**), and (b) 3-carboxy-PROXYL (**2**), both at a collision energy of 20 eV (in the laboratory frame), showing methyl radical loss to form nitrones at *m/z* 184 and 170, respectively.

consecutive losses of methyl radicals rather than a single concerted loss of 30 Da. This stepwise process is illustrated in Scheme 3 and involves an initial loss of the methyl group from the methoxyamine to yield the nitroxide radical that subsequently ejects a methyl group from the piperidine ring. A plausible structure for the ion at *m/z* 184 is therefore the nitrone 4-carboxy-2,2,6-trimethyl-2,3,4,5-tetrahydropyridine-*N*-oxide (Scheme 3a).

An analogous, stepwise methyl radical ejection process is proposed for the dissociation of the 5-membered cyclic nitroxide **2** (Fig. 2b). When the primary ions (*m/z* 185) from O—C homolysis of **2a** are further interrogated by MS^3, ions at *m/z* 170 are observed as a result of methyl radical ejection. A prominent ion at *m/z* 126 is also observed corresponding to the loss of CO_2 from ions at *m/z* 170 and suggesting the carbanion structure as indicated in Scheme 3(b). Formation of this carbanion is facilitated in the PROXYL scaffold by resonance stabilisation by the C=N double bond. This contention is supported by the fact that, decarboxylation is not observed directly from the precursor ion and likewise, CO_2 loss is observed only to a very minor extent (*e.g.* *m/z* 140, Fig. 2a) upon the dissociation of the larger rings of TEMPO-based series where similar stabilisation of the carbanion is not possible.

At high collision energies (E_{lab} > 20 eV), additional low mass ions are observed in the CID spectra of both alkoxyamines **1a** and **2a** (Supporting Information, Fig. S2). Putative structures for these ions are provided as Supporting Information (Scheme S1 and Table S2). Importantly, the presence of these ions in the CID spectra of the authentic nitroxides **1** (*e.g.* *m/z* 122, Fig. 2a) and **2** (*e.g.* *m/z* 108, Fig. 2b) implies that they are secondary dissociation products upon O—C homolysis of alkoxyamines. As secondary product ions, the abundance of these species may be included when considering the total population of ions arising from O—C homolysis at high collision energies.

In Fig. 1, product ions at *m/z* 199 and 184 upon collisional activation of **1a** (and equivalently *m/z* 185 and 170 for **2a**) result from homolysis of the O—C bond. Conversely, ions at *m/z* 183 and 168 are the products of N—O bond cleavage. Homolysis of this bond results in loss of a methoxyl radical, and transient aminyl radicals are observed in low abundance at *m/z* 183 (**1a**), and *m/z* 169 (**2a**). As with the nitroxyl radical product ions, a further loss of 15 Da is also observed in the spectrum, and is likewise assigned to subsequent methyl radical ejection from the aminyl radical to form an imine (Scheme 3). Unlike stable nitroxyl radicals, authentic aminyl radicals are not readily prepared and isolated in the gas phase so CID spectra of known standards were not available for comparison. However, when the primary ions at *m/z* 183 from N—O homolysis of **1a** are isolated in a linear ion trap, product ions at *m/z* 168 are observed in the MS^3 spectrum, arising from facile demethylation of the aminyl radical, even when no additional collisional activation is applied. No significant low mass secondary product ions are identified from further isolation and fragmentation of ions at either *m/z* 183 or 168. When the equivalent primary ions (*m/z* 169) from N—O homolysis of **2a** are analysed by MS^3, ions at *m/z* 154 are similarly observed, indicating subsequent demethylation. An additional ion at *m/z* 110 is also observed, putatively assigned to decarboxylation of *m/z* 154 ions, and resonance stabilised by the C=N double bond. Like the dissociation *via* O—C homolysis, decarboxylation is not observed directly from the precursor ion.

The major product ions observed upon collisional activation of methoxyamine **1a** are summarised in Scheme 3(a). Importantly, product ions at *m/z* 199 and *m/z* 184 are a consequence of O—C homolysis, and *m/z* 183 and *m/z* 168 are the result of N—O homolysis. Equivalent mechanisms are proposed in Scheme 3(b) for the fragmentation of the pyrrolidine-based alkoxyamine **2a**.

3.2. Effect of O-ether functionality (R^3)

Product ions attributed to either N—O or O—C homolysis, as summarised in Scheme 3, do not contain the original *O*-ether fragment (R^3). CID spectra of additional TEMPO-based alkoxyamines **1b–1i**, each with a different R^3 functionality, were also examined (Table 1). In each case, the same product ions were observed as for **1a**, with the spectra only differing in peak intensities. For example, the CID spectra of **1b**, **1g**, **1h**, and **1i** (Fig. 3) all show features at *m/z* 168, 183, 184 and 199 identical to those of **1a** (Fig. 1a). In a similar way, most of the product ions observed for the methoxyamine **2a** (Fig. 1b) are also observed in the CID mass spectra of the PROXYL-based alkoxyamines **2b** and **2h** (Table 1). Significantly, the major product ions arising from dissociation of both series of alkoxyamines do not contain the R^3 substituent (full suite of MS/MS spectra are provided as Supporting Information, Fig. S3).

Product ions not assigned to either N—O or O—C homolysis are observed in the CID spectra of **1h** (Fig. 3c), **2h**, and particularly **1i** (Fig. 3d) to an extent not observed in other substrates. These ions may arise from even-electron dissociation of the precursor ion that is competitive with homolysis when the latter is energetically

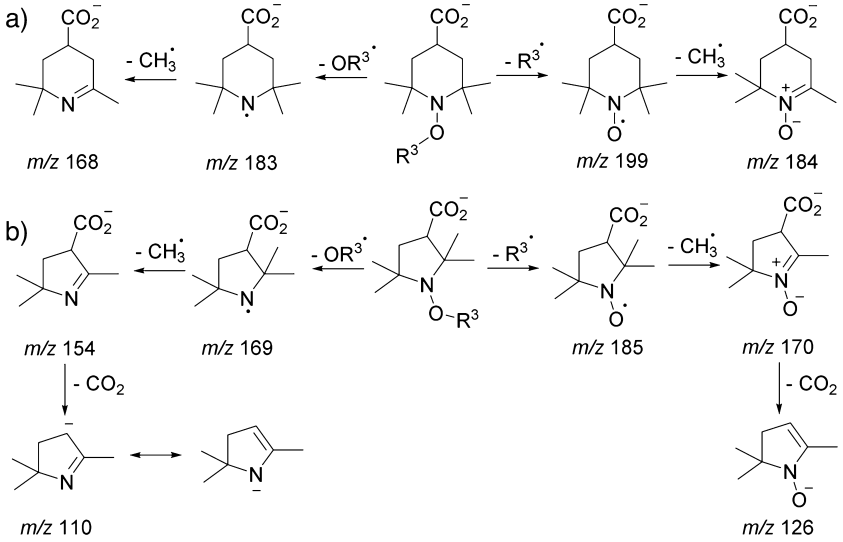

Scheme 3. Stepwise dissociation of negatively charged alkoxyamines through competing charge-remote O—C and N—O homolysis pathways: (a) TEMPO-based alkoxyamines; (b) PROXYL-based alkoxyamines, highlighting additional decarboxylation step and resonance stabilised product ions.

Table 1
Relative abundance of product ions in the CID spectra of $[M-H]^-$ ions based on 4-carboxy-TEMPO (**1**) and 3-carboxy-PROXYL (**2**) at a laboratory-frame collision energy of 15 eV, normalised to base peak (100%) in each spectrum. Each value is an average of at least 3 measurements, each of which comprise at least 50 individual scans.

(R^3)	$[M-H]^-$	*m/z* 199	*m/z* 184	*m/z* 183	*m/z* 168	Other ions *m/z* (% abundance)
1a (CH_3)	76.6	100.0	6.8	1.5	10.1	
1b (CH_2Ph)	3.9	100.0	2.5	n.d.	n.d.	
1c (cyclohex-2-ene)	2.9	100.0	1.6	n.d.	n.d.	
1d ($CH(CH_3)COOEt$)	4.9	100.0	1.5	n.d.	n.d.	
1e (1-CN-$^cC_6H_{11}$)	23.5	100.0	7.6	n.d.	n.d.	
1f ($^tC_4H_9$)	100.0	66.2	1.1	n.d.	0.7	200 (5.7)[a]
1g ($^nC_4H_9$)	100.0	78.1	4.5	0.9	6.2	
1h (CH_2F)	100.0	0.4	14.2	6.0	36.4	182 (6.1)[b]; 138 (39.2); 49 (10.1)
1i ($CH(CH_3)OAc$)	52.4	8.9	1.1	85.0	100.0	226 (78.6)[c]; 59 (54.2)[c]

	$[M-H]^-$	*m/z* 185	*m/z* 170	*m/z* 169	m/z 154	Other ions *m/z* (% abundance)
2a (CH_3)	23.4	100.0	9.8	1.1	5.3	
2b (CH_2Ph)	0.8	100.0	3.7	n.d.	n.d.	
2h (CH_2F)	100.0	1.2	30.0	14.8	69.2	168 (1.8)[b]; 128 (8.2); 110 (3.3); 49 (25.9)

n.d.: less than 0.2% relative to base peak.
[a] Isobutene loss from **1f** (−56 Da).
[b] Concerted loss of HF and formaldehyde from **1h** and **2h**.
[c] *cis*-Elimination from **1i** producing either acetate anion (*m/z* 59) or $[M-CH_3CO_2H]^-$ (*m/z* 226). See text for details.

cumbersome. We speculate that the abundance of N—O homolysis product ions (*m/z* 168 and 183, Fig. 3d) are inflated by a competing charge-remote *cis*-elimination [77] of acetic acid that forms a vinyl-substituted alkoxyamine at *m/z* 226 ($R^1R^2NOCH{=}CH_2$), which then undergoes further dissociation *via* N—O homolysis. When this ion is isolated within the linear ion trap and subjected to further collisional activation in an MS^3 experiment, product ions at *m/z* 183 and *m/z* 168 are observed in high abundance. Due to this competing even-electron dissociation, **1i** is excluded from further discussion on homolysis trends in alkoxyamines.

Based on the product characterisation conducted for **1a**, the product ion at *m/z* 199 in all spectra in Fig. 3 is assigned as 4-carboxy-TEMPO (**1**), arising from homolysis of the O—C bond, and loss of a carbon-centred radical. More generally, homolysis of the O—C bond is a major fragmentation process in the CID of charge-remote alkoxyamines, with a particularly high efficacy in substrates that produce a stabilised alkyl radical (*e.g.* a benzyl radical from **1b** and **2b**, an allyl radical from **1c**, or an α-carbonyl radical from **1d**, **1e**). These results are consistent with the observation of selective O—C bond homolysis upon collisional activation of peptide ions modified with a TEMPO-CH_2Ph linkage [44], structurally similar to **1b**. Conversely, homolysis of the O—C bond is suppressed in **1h** and **2h**, due to anomeric stabilisation of the bond by hyper-conjugation from the adjacent heteroatom [21,37], and thus ions resulting from N—O homolysis are observed in high abundance from these precursors.

3.3. Dissociation thresholds of alkoxyamine ions

The data set presented in Table 1 demonstrate that the alkoxyamine substituent, R^3, influences the relative efficacy of N—O bond homolysis against O—C bond homolysis, which manifests as varying abundances of the ion pairs: *m/z* 168 and 183 for the former, and *m/z* 184 and 199 for the latter (Scheme 3). To explore this effect, the energy acquired by each precursor ion was varied by adjusting the potential difference between the ion source and the collision cell (E_{lab}) of the triple quadrupole mass spectrometer. The normalised abundance of O—C and N—O homolysis product ions were then plotted as a function of applied energy in the centre-of-mass frame (E_{cm}) such that dissociation thresholds (the energy required for formation of 5% product ion abundance, $E_{5\%}$) could be compared between N—O and O—C bonds in a single substrate, and between different substituted alkoxyamines.

For the TEMPO-based alkoxyamines **1a–1h**, cleavage of the O—C bond was found to be the preferred homolysis channel. For example, the aforementioned ions at *m/z* 199 and 184 (and at higher energies, *m/z* 122 and 106 – Fig. 2a) are major product ions in the CID spectrum of methoxypiperidine **1a**, when $E_{cm} > 1.5$ eV ($E_{5\%}$), whereupon dissociation of the precursor ion becomes significant (Fig. 4). The abundance of product ions reaches a maximum at approximately 3.0 eV where they constitute *ca.* 82% of the total ion population. Product ions from N—O homolysis at *m/z* 183 and 168 are observed only at low abundance, accounting for *ca.* 18% of the total ion population, even at the highest energies utilised, with a higher dissociation threshold of 2.3 eV.

The relative dissociation thresholds are rationalised by comparing the calculated free energies of the two bonds. Our results computed at 298 K are given in Fig. 5, while Table S3 in the Supporting Information demonstrates that the qualitative trends in these bond dissociation free energies are largely independent of temperature. In neutral alkoxyamines, O—C homolysis is preferential to N—O homolysis for all R^3 except **1h**, **2h** and **1i** due to anomeric stabilisation of the O—C bond in these three species. The preference for direct O—C cleavage is minimal for those R^3 units that produce relatively non-stabilised carbon-centred radicals upon homolysis, *e.g.* $^{\bullet}CH_3$ and $^t Bu^{\bullet}$ as in **1a**, **1f** and **2a**. However, the most striking feature of Fig. 5 is the effect of deprotonation on these bond homolysis energetics. There is generally no appreciable difference in the N—O bond energetics between neutral and anionic alkoxyamines; however, O—C bonds are significantly weakened toward homolytic cleavage by deprotonation of the remote carboxylic acid moiety. This is due to a combination of two factors: (i) conventional polar effect of the negative charge destabilising alkoxyamines and stabilising the forming nitroxyl *via* their corresponding charge-separated resonance contributors, $R^1R^2NO^-—R^{3+}$ and $R^1R^2N^{+\bullet}—O^-$, respectively; and (ii) additional Coulombic stabilisation of nitroxyl radicals by remote negative charges arising from their enhanced polarisability [65,68]. Based on these arguments, we predict that inverting the charge polarity would strengthen the O—C bond due to these polar effects. Relocating the charge site onto the opposite side of the O—C bond (as in TEMPO-mediated peptide sequencing) would minimise the latter stabilisation contribution due to the lower alkyl radical

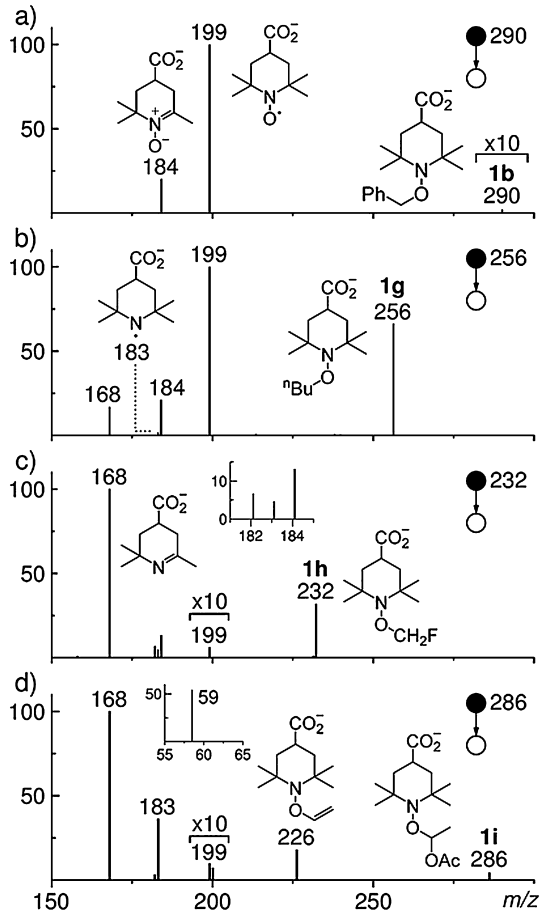

Fig. 3. Negative ion CID MS/MS spectra (at a collision energy of 20 eV) of alkoxyamines, each exhibiting varying abundances of product ions at m/z 184, 183, and 168; (a) benzyloxyamine **1b**, (b) *n*-butyloxyamine **1g**, (c) fluoromethoxyamine **1h** (a minor ion at m/z 182 is assigned to loss of HF and CH_2O), (d) (1-acetyloxy) ethoxyamine **1i**, which also undergoes *cis*-elimination to produce vinyloxyamine (m/z 226) and acetate ions (m/z 59).

polarisability relative to a nitroxyl radical [68]. Moreover, with respect to polar resonance contributors, a negative charge on the R^3 substituent would be expected to raise the O—C bond energy whereas a positive charge would decrease the bond energy [46,68]. The thermodynamic preference ($\Delta\Delta G_{298}$) for O—C cleavage in deprotonated alkoxyamines in the present investigation is further

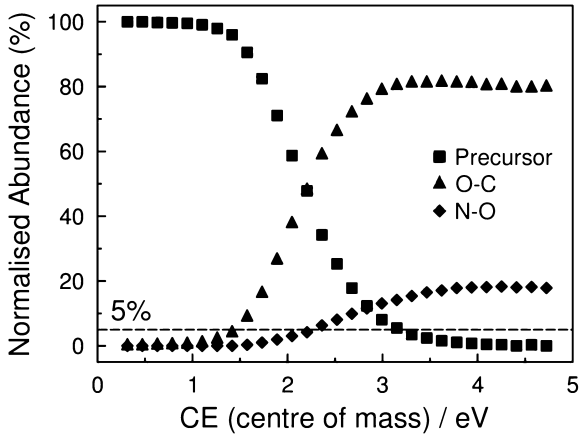

Fig. 4. Relative abundance of product ions arising from N—O homolysis and O—C homolysis of methoxypiperidine (**1a**) as a function of applied collision energy in the centre-of-mass frame.

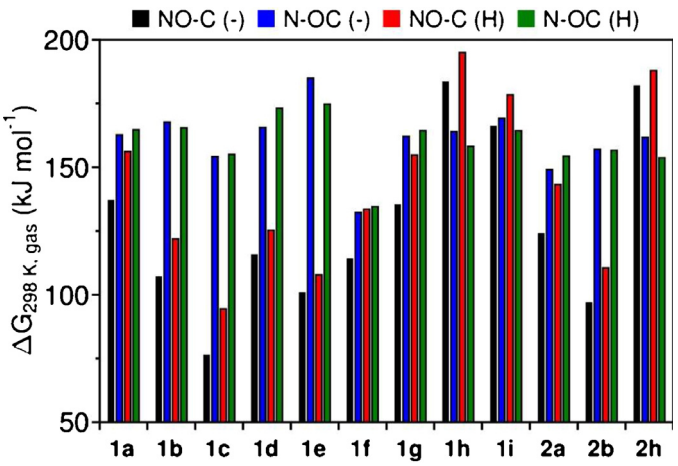

Fig. 5. Calculated free energies (kJ mol^{-1}) of O—C and N—O bond homolysis in anionic (−) and neutral (H) alkoxyamines at 298 K.

enhanced by up to 20 kJ mol^{-1} compared to their neutral counterparts. This observation is true for all R^3 moieties studied herein, and thus trends in the effect of the R^3 moiety are representative of the trends in neutral species.

Breakdown curves for the alkoxyamines **1b–1e** are shown in Fig. 6(a). Homolysis of the O—C bond occurs at a significantly lower threshold energy ($E_{5\%}$ = 0.5–0.7 eV) compared to methoxyamine **1a** ($E_{5\%}$ = 1.5 eV). In these substrates, almost quantitative conversion from alkoxyamine to nitroxyl radical is observed, even below collision energies of 2.0 eV. Furthermore, O—C homolysis is highly selective, with no N—O homolysis product ions detected at m/z 168 or 183 for any of the precursors **1b–1e**. Compared to the alkyl ethers (*e.g.* **1a**, **1f**, **1g**), which exhibit a modest thermodynamic preference for homolysis of the O—C bond, substrates **1b–1e** contain much weaker O—C bonds ($\Delta G_{298} < 120$ kJ mol^{-1}), and a greater selectivity ($\Delta\Delta G_{298} > 60$ kJ mol^{-1}) for O—C cleavage (Fig. 5). These observations are consistent with the presence of R^3-substituents that stabilise the resulting alkyl radical for **1b–1e**.

Conversely, the alkoxyamine containing an adjacent heteroatom (**1h**) exhibits remarkably different fragmentation behaviour. In Fig. 6(b), the O—C homolysis product ion abundance from the CID of **1h** (and **1a**, for comparison) are plotted with open shapes, whilst the abundance of corresponding N—O product ions are denoted with filled shapes. In **1h**, there is competition between the two pathways much like the alkyl substituted alkoxyamine **1a**, however in this case N—O homolysis is the dominant pathway, and products of O—C homolysis are observed in minor abundance. Despite this, selectivity is not as pronounced as in **1b–1e**. Furthermore, higher experimental threshold energies are required for dissociation of the N—O bond: 1.8 eV for **1h** and 2.3 eV for **1a**, compared with 1.5 eV for O—C homolysis in **1a**. These observations are rationalised by again considering the relative N—O and O—C bond energies in these ions (Fig. 5). In deprotonated **1h**, the free energy required to cleave either the N—O (163.9 kJ mol^{-1}) or O—C bonds (183.6 kJ mol^{-1}) at 298 K is higher than the energy requirement for cleavage of the O—C bonds in substrates that preferentially dissociate *via* O—C homolysis (75–135 kJ mol^{-1}).

Within the current experiment it is also possible to compare homolytic dissociation not only as a function of *O*-ether alkoxyamine substituent, but also as a function of ring size, by comparing the breakdown curves of 6-membered cyclic alkoxyamines (**1x**) with the equivalent 5-membered rings (**2x**). In Fig. 7, breakdown curves show the normalised abundances of ions arising from O—C homolysis of TEMPO-based **1a**, **1b**, **1h** (denoted by open shapes), as well as PROXYL-based **2a**, **2b** and **2h** (filled shapes). Compared to

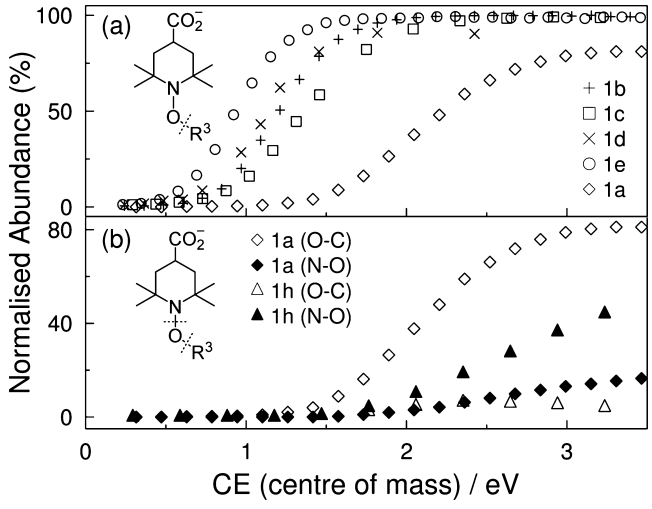

Fig. 6. (a) Selective O—C homolysis in alkoxyamines (**1b–1e**) that release a stable radical upon dissociation. (b) N—O homolysis (filled shapes) is the dominant fragmentation mechanism upon CID of fluoromethoxyamine (**1h**). Methoxyamine (**1a**) is included for comparison, exhibiting preference for O—C cleavage (open shapes).

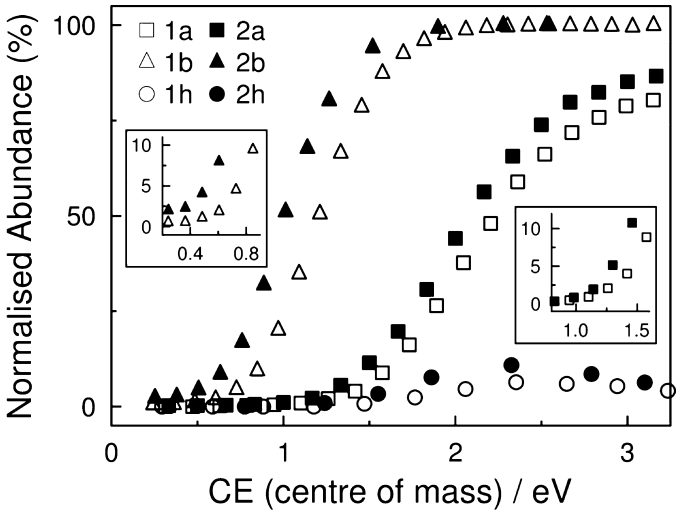

Fig. 7. Breakdown curves comparing O—C homolysis in 6-membered TEMPO-based alkoxyamines (open shapes) with the more facile homolysis in 5-membered PROXYL-based alkoxyamines (filled shapes), with methyl, benzyl, and fluoromethyl substituents. A lower threshold energy is required for dissociating alkoxyamines based on the PROXYL ring (see insets), compared to TEMPO, a trend reflected in the relative O—C bond energies (Fig. 5).

TEMPO-based alkoxyamines, PROXYL-based alkoxyamines exhibit a greater overall abundance of product ions at a given collision energy input, and similarly a lower O—C dissociation threshold (*e.g.* 1.2 eV for **2a** and 0.5 eV for **2b**, compared with 1.5 eV for **1a** and 0.7 eV for **1b**). Both O—C and N—O bonds are systematically weaker in 5-membered PROXYL-based alkoxyamines, compared with equivalent 6-membered TEMPO-based alkoxyamines, resulting in more facile dissociation. For the methyl and benzyl substituents, the calculated O—C bond dissociation free energy is 10–13 kJ mol^{-1} lower in PROXYL substrates compared to TEMPO (Fig. 5), consistent with the observation of lower experimental threshold energies. When the alkoxyamine contains the fluoromethyl moiety, the O—C bonds of **1h** and **2h** are approximately isoenergetic, thus the similarity in their dissociation thresholds.

By combining all of the obtained experimental and computational data from both TEMPO and PROXYL-based alkoxyamines, the utility of this method for experimentally deriving relative thermodynamic quantities can be evaluated. There is a good correlation (R^2 = 0.82, Supporting Information Fig. S4) between experimentally obtained O—C threshold energies and calculated gas phase free energies of O—C homolysis. The fit spans an energy range of over 150 kJ mol^{-1}, from substrates with weak O—C bonds due to the formation of stable carbon-centred radicals upon dissociation (*e.g.* **1b–1e**), to those with anomeric stabilisation of their O—C bonds (**1h**). However, the experimental dissociation threshold values are systematically over-estimated with respect to the calculated bond dissociation free energies (slope = 0.6, intercept = 62 kJ mol^{-1}). This offset indicates a significant kinetic shift [78,79], which is the excess energy required to produce detectable dissociation of an ion within the experimental timeframe, and scales with increasing vibrational degrees of freedom. That is, the observed dissociation threshold is only an upper limit to the true thermochemical value. Moreover, when N—O homolysis is energetically competitive with O—C homolysis, a competitive shift may inhibit formation of higher-energy products, and as such are detected only at energies above the actual thresholds [80]. In these experiments, conducted on a commercial triple quadrupole mass spectrometer, the initial energy distribution and the kinetic energy of the ion population is not adequately controlled. This stands in contrast to guided ion beam mass spectrometry, wherein these parameters are precisely controlled and thus the resulting data can be used to derive accurate thermochemical quantities [81,82]. Despite these limitations, for the aims of the current work, the experimentally derived dissociation thresholds have provided an excellent means to explore relative trends in bond energies and to test computational predictions.

4. Conclusions

A suite of novel alkoxyamines was prepared based on the nitroxyl radicals 4-carboxy-TEMPO (**1**) and 3-carboxy-PROXYL (**2**). CID of $[M-H]^-$ anions in a triple quadrupole mass spectrometer produced radical fragment ions, which arise from charge-remote homolysis of either the O—C or N—O bonds. The relative abundance of these ions is dependent on the *O*-alkyl functionality. These systems thus allowed the first direct experimental comparison of the competition between O—C and N—O homolysis in alkoxyamines. An exception to this behaviour was observed for alkoxyamine **1i**, in which a charge-remote electrocyclic rearrangement was competitive with homolysis.

Breakdown curves were utilised to experimentally compare dissociation thresholds. The majority of alkoxyamines exhibit an O—C dissociation threshold lower than their corresponding N—O dissociation threshold, consistent with their relative calculated bond dissociation free energies. Only in the presence of a fluoromethyl substituent (**1h** and **2h**) was N—O cleavage unequivocally observed as the dominant dissociation mechanism. Calculations further reveal that – compared with neutral scaffolds – O—C bonds are weakened in the presence of a negative charge on the TEMPO or PROXYL ring by *ca.* 20 kJ mol^{-1} [65,68]. However, the effect is consistent across the range of scaffolds studied, and thus the observed structural trends are also representative of neutral alkoxyamines.

In controlled radical polymerisation and polymer stabilisation, the *O*-ether substituent (R^3) is dependent on the radicals produced by the growing or degrading polymer substrate. For example, benzyloxyamines (**1b** and **2b**) are models for the alkoxyamines derived from polystyrenes, whereas carbonyl-containing substrates (**1c** and **1i**) represent the capture of model polyester-derived radicals. It is clear from the presented data that direct N—O homolysis is typically not competitive with the prevailing O—C homolysis. Only in the presence of an adjacent heteroatom would N—O homolysis be expected to dominate. Therefore, aminyl

radicals and secondary amines observed in the degradation of alkoxyamines at normal service temperatures (up to 80 °C) are likely not formed directly from N—O bond homolysis, but by alternative processes, such as those outlined in Scheme 1(a) [12,13].

Acknowledgements

The authors acknowledge the generous financial assistance provided by the Australian Research Council (ARC) through the Centre of Excellence for Free Radical Chemistry and Biotechnology (CE0561607) and Discovery grants (DP140101237) schemes, an ARC Future Fellowship (to M.L.C.), an Australian Postgraduate Award (to D.L.M.), and allocations of supercomputing time on the National Facility of the Australian National Computational Infrastructure.

Appendix A. Supplementary data

Supplementary data associated with this article can be found, in the online version, at http://dx.doi.org/10.1016/j.ijms.2014.06.030.

References

[1] F. Gugumus, The performance of light stabilizers in accelerated and natural weathering, Polym. Degrad. Stab. 50 (1995) 101–116.
[2] C. Schaller, D. Rogez, A. Braig, Hindered amine light stabilizers in pigmented coatings, J. Coat. Technol. Res. 6 (2009) 81–88.
[3] J.L. Hodgson, M.L. Coote, Clarifying the mechanism of the Denisov cycle: how do hindered amine light stabilizers protect polymer coatings from photo-oxidative degradation? Macromolecules 43 (2010) 4573–4583.
[4] P. Gijsman, J. Hennekens, D. Tummers, The mechanism of action of hindered amine light stabilizers, Polym. Degrad. Stab. 39 (1993) 225–233.
[5] P.P. Klemchuk, M.E. Gande, E. Cordola, Hindered amine mechanisms: Part III—Investigations using isotopic labelling, Polym. Degrad. Stab. 27 (1990) 65–74.
[6] D.R. Bauer, J.L. Gerlock, D.F. Mielewski, Photo-degradation and photo-stabilization in organic coatings containing a hindered amine light stabilizer: Part VI—ESR measurements of nitroxide kinetics and mechanism of stabilization, Polym. Degrad. Stab. 28 (1990) 115–129.
[7] J. Pospišil, S. Nešpurek, Photostabilization of coatings. Mechanisms and performance, Prog. Polym. Sci. 25 (2000) 1261–1335.
[8] F. Gugumus, Mechanisms and kinetics of photostabilization of polyolefins with HALS, Die Angew. Makromol. Chem. 176/177 (1990) 241–289.
[9] K. Schwetlick, W.D. Habicher, Antioxidant action mechanisms of hindered amine stabilisers, Polym. Degrad. Stab. 78 (2002) 35–40.
[10] E.N. Step, N.J. Turro, M.E. Gande, P.P. Klemchuk, Mechanism of polymer stabilization by hindered-amine light stabilizers (HALS) – model investigations of the interaction of peroxy-radicals with HALS amines and amino ethers, Macromolecules 27 (1994) 2529–2539.
[11] E.N. Step, N.J. Turro, P.P. Klemchuk, M.E. Gande, Model studies on the mechanism of HALS stabilization, Angew. Makromol. Chem. 232 (1995) 65–83.
[12] G. Gryn'ova, K.U. Ingold, M.L. Coote, New insights into the mechanism of amine/nitroxide cycling during the Hindered Amine Light Stabilizer inhibited oxidative degradation of polymers, J. Am. Chem. Soc. 134 (2012) 12979–12988.
[13] M.R.L. Paine, G. Gryn'ova, M.L. Coote, P.J. Barker, S.J. Blanksby, Desorption electrospray ionisation mass spectrometry of stabilised polyesters reveals activation of hindered amine light stabilisers, Polym. Degrad. Stab. 99 (2014) 223–232.
[14] J.M. Cogen, Semiempirical prediction of the thermochemistry of intermediates involved in the cyclic mechanism of hindered amine stabilizers, Polym. Degrad. Stab. 44 (1994) 49–53.
[15] J.L. Hodgson, L.B. Roskop, M.S. Gordon, C.Y. Lin, M.L. Coote, Side reactions of Nitroxide-Mediated Polymerization: N-O versus O-C cleavage of alkoxyamines, J. Phys. Chem. A 114 (2010) 10458–10466.
[16] C.J. Hawker, A.W. Bosman, E. Harth, New polymer synthesis by nitroxide mediated living radical polymerizations, Chem. Rev. 101 (2001) 3661–3688.
[17] C.J. Hawker, Molecular-weight control by a living free-radical polymerization process, J. Am. Chem. Soc. 116 (1994) 11185–11186.
[18] G. Moad, E. Rizzardo, S.H. Thang, Toward living radical polymerization, Acc. Chem. Res. 41 (2008) 1133–1142.
[19] G. Gryn'ova, C.Y. Lin, M.L. Coote, Which side-reactions compromise nitroxide mediated polymerization? Polym. Chem. 4 (2013) 3744–3754.
[20] S.R.A. Marque, Influence of the nitroxide structure on the homolysis rate constant of alkoxyamines: A Taft-Ingold analysis, J. Org. Chem. 68 (2003) 7582–7590.
[21] S.R.A. Marque, H. Fischer, E. Baier, A. Studer, Factors influencing the C-O bond homolysis of alkoxyamines: effects of H-bonding and polar substituents, J. Org Chem. 66 (2001) 1146–1156.
[22] S.R.A. Marque, C. Le Mercier, P. Tordo, H. Fischer, Factors influencing the C-O bond homolysis of trialkylhydroxylamines, Macromolecules 33 (2000) 4403–4410.
[23] D. Bertin, D. Gigmes, S.R.A. Marque, P. Tordo, Polar, steric, and stabilization effects in alkoxyamines C-ON bond homolysis: a multiparameter analysis, Macromolecules 38 (2005) 2638–2650.
[24] G.S. Ananchenko, H. Fischer, Decomposition of model alkoxyamines in simple and polymerizing systems. I. 2,2,6,6-tetramethylpiperidinyl-*N*-oxyl-based compounds, J. Polym. Sci. Part A: Polym. Chem. 39 (2001) 3604–3621.
[25] P. Marsal, M. Roche, P. Tordo, P. de Sainte Claire, Thermal stability of O–H and O–alkyl bonds in *N*-alkoxyamines. A density functional theory approach, J. Phys. Chem. A 103 (1999) 2899–2905.
[26] G. Moad, E. Rizzardo, Alkoxyamine-initiated living radical polymerization: factors affecting alkoxyamine homolysis rates, Macromolecules 28 (1995) 8722–8728.
[27] J.L. Hodgson, C.Y. Lin, M.L. Coote, S.R.A. Marque, K. Matyjaszewski, Linear free-energy relationships for the alkyl radical affinities of nitroxides: a theoretical study, Macromolecules 43 (2010) 3728–3743.
[28] C.Y. Lin, S.R.A. Marque, K. Matyjaszewski, M.L. Coote, Linear-free energy relationships for modeling structure-reactivity trends in controlled radical polymerization, Macromolecules 44 (2011) 7568–7583.
[29] D. Gigmes, A. Gaudel-Siri, S.R.A. Marque, D. Bertin, P. Tordo, P. Astolfi, L. Greci, C. Rizzoli, Alkoxyamines of stable aromatic nitroxides: N-O vs. C-O bond homolysis, Helv. Chim. Acta 89 (2006) 2312–2326.
[30] Y. Guillaneuf, D. Bertin, D. Gigmes, D.-L. Versace, J. Lalevee, J.-P. Fouassier, Toward nitroxide-mediated photopolymerization, Macromolecules 43 (2010) 2204–2212.
[31] D.-L. Versace, Y. Guillaneuf, D. Bertin, J.P. Fouassier, J. Lalevee, D. Gigmes, Structural effects on the photodissociation of alkoxyamines, Org. Biomol. Chem. 9 (2011) 2892–2898.
[32] J.W. Grissom, G.U. Gunawardena, Intermolecular reaction of nitroxide radicals with biradical intermediates generated from aromatic enediynes, Tetrahedron Lett. 36 (1995) 4951–4954.
[33] H. Henry-Riyad, T.T. Tidwell, Thermolysis of *N*-tetramethylpiperidinyl triphenylacetate: homolytic fragmentation of a TEMPO ester, J. Phys. Org. Chem. 16 (2003) 559–563.
[34] W.W. Huang, H. Henry-Riyad, T.T. Tidwell, Reactions of the "stable" nitroxyl radical TEMPO with ketenes: formation of a unique peroxidic source of aminyl radicals, J. Am. Chem. Soc. 121 (1999) 3939–3943.
[35] J.L. Heidbrink, F.S. Amegayibor, H.I. Kenttämaa, Gas-phase radical–radical recombination reactions of nitroxides with substituted phenyl radicals, Int. J. Chem. Kinet. 36 (2004) 216–229.
[36] A. Gaudel-Siri, D. Siri, P. Tordo, Homolysis of *N*-alkoxyamines: a computational study, ChemPhysChem 7 (2006) 430–438.
[37] M.V. Ciriano, H.-G. Korth, W.B. van Scheppingen, P. Mulder, Thermal stability of 2,2,6,6-tetramethylpiperidine-1-oxyl (TEMPO) and related *N*-alkoxyamines, J. Am. Chem. Soc. 121 (1999) 6375–6381.
[38] J. Adams, M.L. Gross, Charge-remote fragmentations of closed-shell ions. A thermolytic analogy, J. Am. Chem. Soc. 111 (1989) 435–440.
[39] C.F. Cheng, M.L. Gross, Applications and mechanisms of charge-remote fragmentation, Mass Spectrom. Rev. 19 (2000) 398–420.
[40] S. Dua, J.H. Bowie, B.A. Cerda, C. Wesdemiotis, Search for charge-remote reactions of even-electron organic negative ions in the gas phase. Anions derived from disubstituted adamantanes, J. Chem. Soc Perkin Trans. 2 (1998) 1443–1448.
[41] I.C. Wienhöfer, H. Luftmann, A. Studer, Nitroxide-mediated copolymerization of MMA with styrene: sequence analysis of oligomers by using mass spectrometry, Macromolecules 44 (2011) 2510–2523.
[42] P.J. Wright, A.M. English, Scavenging with TEMPO to identify peptide- and protein-based radicals by mass spectrometry: advantages of spin scavenging over spin trapping, J. Am. Chem. Soc. 125 (2003) 8655–8665.
[43] M. Berger, J. Cadet, J. Ulrich, Radiation-induced binding of 2,2,6,6-tetramethyl-1,4-piperidone-*N*-oxyl to thymidine in oxygen-free aqueous solutions. Isolation and characterization of the adducts, Can. J. Chem. 63 (1985) 6–14.
[44] M. Lee, M. Kang, B. Moon, H.B. Oh, Gas-phase peptide sequencing by TEMPO-mediated radical generation, Analyst 134 (2009) 1706–1712.
[45] M. Lee, Y. Lee, M. Kang, H. Park, Y. Seong, B.J. Sung, B. Moon, H.B. Oh, Disulfide bond cleavage in TEMPO-free radical initiated peptide sequencing mass spectrometry, J. Mass Spectrom. 46 (2011) 830–839.
[46] J. Lee, H. Park, H. Kwon, G. Kwon, A. Jeon, H.I. Kim, B.J. Sung, B. Moon, H. Oh, One-step peptide backbone dissociations in negative-ion free radical initiated peptide sequencing mass spectrometry, Anal. Chem. 85 (2013) 7044–7051.
[47] X. Zhang, H. Wang, Y. Guo, Interception of the radicals produced in electrophilic fluorination with radical traps (TEMPO, DMPO) studied by electrospray ionization mass spectrometry, Rapid Commun. Mass Spectrom. 20 (2006) 1877–1882.
[48] T.A. Lowe, M.R.L. Paine, D.L. Marshall, L.A. Hick, J.A. Boge, P.J. Barker, S.J. Blanksby, Structural identification of hindered amine light stabilisers in coil coatings using electrospray ionisation tandem mass spectrometry, J. Mass Spectrom. 45 (2010) 486–495.
[49] C. Tansakul, E. Lilie, E.D. Walter, F. Rivera, A. Wolcott, J.Z. Zhang, G.L. Millhauser, R. Braslau, Distance-dependent fluorescence quenching and binding of CdSe quantum dots by functionalized nitroxide radicals, J. Phys. Chem. C 114 (2010) 7793–7805.
[50] S. Harrisson, P. Couvreur, J. Nicolas, Simple and efficient copper metal-mediated synthesis of alkoxyamine initiators, Polym. Chem. 2 (2011) 1859–1865.
[51] K. Matyjaszewski, B.E. Woodworth, X. Zhang, S.G. Gaynor, Z. Metzner, Simple and efficient synthesis of various alkoxyamines for stable free radical polymerization, Macromolecules 31 (1998) 5955–5957.

[52] T.J. Connolly, M.V. Baldovi, N. Mohtat, J.C. Scaiano, Photochemical synthesis of TEMPO-capped initiators for "living" free radical polymerization, Tetrahedron Lett. 37 (1996) 4919–4922.
[53] Y. Miura, K. Hirota, H. Moto, B. Yamada, High-yield synthesis of alkoxyamine initiators carrying a functional group by reaction of ethylbenzenes with di-tert-butyl diperoxalate in the presence of nitroxides, Macromolecules 31 (1998) 4659–4661.
[54] R. Braslau, A. Tsimelzon, J. Gewandter, Novel methodology for the synthesis of *N*-alkoxyamines, Org. Lett. 6 (2004) 2233–2235.
[55] K.-U. Schoening, W. Fischer, S. Hauck, A. Dichtl, M. Kuepfert, Synthetic studies on *N*-alkoxyamines: a mild and broadly applicable route starting from nitroxide radicals and aldehydes, J. Org. Chem. 74 (2008) 1567–1573.
[56] A. Dichtl, M. Seyfried, K.U. Schoening, A novel method for the synthesis of *N*-alkoxyamines starting from nitroxide radicals and ketones, Synlett (2008) 1877–1881.
[57] J.E. Babiarz, G.T. Cunkle, A.D. DeBellis, D. Eveland, S.D. Pastor, S.P. Shum, The thermal reaction of sterically hindered nitroxyl radicals with allylic and benzylic substrates: experimental and computational evidence for divergent mechanisms, J. Org Chem. 67 (2002) 6831–6834.
[58] S. Coseri, K.U. Ingold, Distinguishing between abstraction and addition as the first step in the reaction of a nitroxyl radical with cyclohexene, Org. Lett. 6 (2004) 1641–1643.
[59] E.G. Rozantsev, V.D. Sholle, Synthesis and reactions of stable nitroxyl radicals II. Reactions 1, Synthesis 1971 (1971) 401–414.
[60] V. Strehmel, H. Rexhausen, P. Strauch, Synthesis of 4-trimethylammonio-2,2,6,6-tetramethylpiperidine-1-yloxyl with various anions for investigation of ionic liquids, Tetrahedron Lett. 49 (2008) 3264–3267.
[61] D. Schröder, M. Engeser, M. Brönstrup, C. Daniel, J. Spandl, H. Hartl, Ion chemistry of the hexanuclear methoxo-oxovanadium cluster $V_6O_7(OCH_3)_{12}$, Int. J. Mass Spectrom. 228 (2003) 743–757.
[62] D. Schröder, M. Engeser, H. Schwarz, E. Rosenthal, J. Döbler, J. Sauer, Degradation of ionized $OV(OCH_3)_3$ in the gas phase. From the neutral compound all the way down to the quasi-terminal fragments VO^+ and VOH^+, Inorg. Chem. 45 (2006) 6235–6245.
[63] M.J. Frisch, G.W. Trucks, H.B. Schlegel, G.E. Scuseria, M.A. Robb, J.R. Cheeseman, G. Scalmani, V. Barone, B. Mennucci, G.A. Petersson, H. Nakatsuji, M. Caricato, X. Li, H.P. Hratchian, A.F. Izmaylov, J. Bloino, G. Zheng, J.L. Sonnenberg, M. Hada, M. Ehara, K. Toyota, R. Fukuda, J. Hasegawa, M. Ishida, T. Nakajima, Y. Honda, O. Kitao, H. Nakai, T. Vreven, J.A. Montgomery, J.E. Peralta, F. Ogliaro, M. Bearpark, J.J. Heyd, E. Brothers, K.N. Kudin, V.N. Staroverov, R. Kobayashi, J. Normand, K. Raghavachari, A. Rendell, J.C. Burant, S.S. Iyengar, J. Tomasi, M. Cossi, N. Rega, J.M. Millam, M. Klene, J.E. Knox, J.B. Cross, V. Bakken, C. Adamo, J. Jaramillo, R. Gomperts, R.E. Stratmann, O. Yazyev, A.J. Austin, R. Cammi, C. Pomelli, J.W. Ochterski, R.L. Martin, K. Morokuma, V.G. Zakrzewski, G.A. Voth, P. Salvador, J.J. Dannenberg, S. Dapprich, A.D. Daniels, Farkas, J.B. Foresman, J.V. Ortiz, J. Cioslowski, D.J. Fox, Gaussian 09, Revision C.01 (2009).
[64] H.-J. Werner, P.J. Knowles, G. Knizia, F.R. Manby, M. Schütz, P. Celani, T. Korona, R. Lindh, A. Mitrushenkov, G. Rauhut, K.R. Shamasundar, T.B. Adler, R.D. Amos, A. Bernhardsson, A. Berning, D.L. Cooper, M.J.O. Deegan, A.J. Dobbyn, F. Eckert, E. Goll, C. Hampel, A. Hesselman, G. Hetzer, T. Hrenar, G. Jansen, C. Köppl, Y. Liu, A.W. Lloyd, R.A. Mata, A.J. May, S.J. McNicholas, W. Meyer, M.E. Mura, A. Nicklass, D.P. O'Neill, P. Palmieri, D. Peng, K. Pflüger, R. Pitzer, M. Reiher, T. Shizoaki, H. Stoll, A.J. Stone, R. Tarroni, T. Thosteinsson, M. Wang, MOLPRO 2012.1, a package of *ab initio* programs, see http://www.molpro.net (2012).
[65] G. Gryn'ova, D.L. Marshall, S.J. Blanksby, M.L. Coote, Switching radical stability by pH-induced orbital conversion, Nat. Chem. 5 (2013) 474–481.
[66] J.P. Merrick, D. Moran, L. Radom, An evaluation of harmonic vibrational frequency scale factors, J. Phys. Chem. A 111 (2007) 11683–11700.
[67] L.A. Curtiss, K. Raghavachari, P.C. Redfern, A.G. Baboul, J.A. Pople, Gaussian-3 theory using coupled cluster energies, Chem. Phys. Lett. 314 (1999) 101–107.
[68] G. Gryn'ova, M.L. Coote, Origin and scope of long-range stabilizing interactions and associated SOMO-HOMO conversion in distonic radical anions, J. Am. Chem. Soc. 135 (2013) 15392–15403.
[69] J.I. Steinfeld, J.S. Francisco, W.L. Hase, Chemical Kinetics and Dynamics, Prentice Hall, Englewood Cliffs, 1989.
[70] C. Barner-Kowollik, T.P. Davis, M.H. Stenzel, Probing mechanistic features of conventional, catalytic and living free radical polymerizations using soft ionization mass spectrometric techniques, Polymer 45 (2004) 7791–7805.
[71] M.A. Dourges, B. Charleux, J.P. Vairon, J.C. Blais, G. Bolbach, J.C. Tabet, MALDI-TOF mass spectrometry analysis of TEMPO-capped polystyrene, Macromolecules 32 (1999) 2495–2502.
[72] M.R.L. Paine, P.J. Barker, S.A. MacLauglin, T.W. Mitchell, S.J. Blanksby, Direct detection of additives and degradation products from polymers by liquid extraction surface analysis employing chip-based nanospray mass spectrometry, Rapid Commun. Mass Spectrom. 26 (2012) 412–418.
[73] M.R.L. Paine, P.J. Barker, S.J. Blanksby, Desorption electrospray ionisation mass spectrometry reveals in situ modification of a hindered amine light stabiliser resulting from direct N-OR bond cleavage, Analyst 136 (2011) 904–912.
[74] M. Mazarin, M. Girod, S. Viel, T.N.T. Phan, S.R.A. Marque, S. Humbel, L. Charles, Role of the adducted cation in the release of nitroxide end group of controlled polymer in mass spectrometry, Macromolecules 42 (2009) 1849–1859.
[75] M. Karni, A. Mandelbaum, The even-electron rule, Org. Mass Spectrom. 15 (1980) 53–64.
[76] F.W. McLafferty, F. Tureček, Interpretation of Mass Spectra, University Science Books, Mill Valley, 1993.
[77] S. Dua, J.H. Bowie, B.A. Cerda, C. Wesdemiotis, The facile loss of formic acid from an anion system in which the charged and reacting centres cannot interact, Chem. Commun. (1998) 183–184.
[78] S.M. Gordon, N.W. Reid, An investigation of the kinetic shift in mass spectrometry, Int. J. Mass Spectrom. Ion Phys. 18 (1975) 379–391.
[79] C. Lifshitz, Kinetic shifts, Eur. J. Mass Spectrom. 8 (2002) 85–98.
[80] F. Muntean, P.B. Armentrout, Modeling kinetic shifts and competition in threshold collision-induced dissociation. Case study: *n*-butylbenzene cation dissociation, J. Phys. Chem. A 107 (2003) 7413–7422.
[81] P.B. Armentrout, Mass spectrometry – not just a structural tool: the use of guided ion beam tandem mass spectrometry to determine thermochemistry, J. Am. Soc. Mass Spectrom. 13 (2002) 419–434.
[82] P.B. Armentrout, The power of accurate energetics (or thermochemistry: what is it good for?), J. Am. Soc. Mass Spectrom. 24 (2013) 173–185.